

Article

Impact of Annealing Temperature on the Physical Properties of the Lanthanum Deficiency Manganites

Skini Ridha ^{1,*}, Dhahri Essebti ² and El Kebir Hlil ³

¹ Center for Functionalized Magnetic Materials (FunMagMa), Immanuel Kant Baltic Federal University, 236041 Kaliningrad, Russia

² Laboratoire de Physique Appliquée, Faculté des Sciences de Sfax, B.P. 802, Université de Sfax, Sfax 3018, Tunisia; essebtidhahri@yahoo.com

³ Institut Néel, CNRS et Université Joseph Fourier, BP 166, F-38042 Grenoble CEDEX 9, France; el-kebir.hlil@neel.cnrs.fr

* Correspondence: skini.ridha@ymail.com

Academic Editor: Alex V. Morozkin

Received: 20 August 2017; Accepted: 2 October 2017; Published: 5 October 2017

Abstract: The lanthanum deficiency manganites $\text{La}_{0.8-x}\square_x\text{Ca}_{0.2}\text{MnO}_3$ ($x = 0, 0.1$ and 0.2), where \square is a lanthanum vacancy, were prepared using the classic ceramic methods with different thermal treatments (1373 K and 973 K). The structural, magnetic, and magnetocaloric properties of these compounds were studied as a function of annealing temperature. It was noted that the annealing temperature did not affect the crystal structure of our samples (orthorhombic structure with Pnma space group). Nevertheless, a change in the variation of the unit cell volume V , the average bond length $d_{\text{Mn-O}}$, and the average bond angles $\theta_{\text{Mn-O-Mn}}$ were observed. Magnetization versus temperature study has shown that all samples exhibited a magnetic transition from ferromagnetic (FM) to paramagnetic (PM) phase with increasing temperature. However, it can be clearly seen that the annealing at 973 K induced an increase of the magnetization. In addition, the magnetocaloric effect (MCE) as well as the relative cooling power (RCP) were estimated. As an important result, the values of MCE and RCP in our Lanthanum-deficiency manganites are reported to be near to those found in gadolinium, considered as magnetocaloric reference material.

Keywords: vacancy manganites; thermal treatments; magnetocaloric effect

1. Introduction

Magnetic refrigeration technique is one of the most promising techniques in cooling technology due to the efficient and environmentally safe cooling applications, which have encouraged the experimental and the theoretical studies in this direction. Obtaining low-cost and high-performance magnetocaloric materials is not an easy target because of the related drawbacks. For instance, Gd shows a large magnetocaloric effect (MCE) in room temperature range [1], yet it is a costly element which tends to oxidation. Recent research seeks to balance the needs for technical applications by obtaining high magnetocaloric performance with fewer disadvantages by exploring several kinds of magnetic materials treated in different conditions.

In recent times, mixed valence manganites with the general formula $\text{La}_{1-x}\text{A}_x\text{MnO}_3$, where A is a divalent element ($A = \text{Ca}, \text{Sr}, \text{Ba}, \dots$), have roused plenty of research thanks to their important electrical and magnetic properties, such as the colossal magnetoresistance (CMR) [2–8] and the magnetocaloric effect (MCE) [9–14]. That is why the parameter necessary for selecting magnetic refrigerants is based on the cooling power per unit volume and the relative cooling power (RCP). This parameter is a measure of the amount of heat transfer between the cold and hot sinks in a refrigeration cycle, estimating the range of operating temperature.

To ameliorate this parameter, wide-ranging research has been conducted, hence the development of many synthetic methods of producing these materials, such as solid state reaction, sol-gel, coprecipitation, high-energy ball-milling, polyol process, spark plasma sintering, etc.

Other research works have shown that the physical properties of ceramics are also sensitive to the value of the sintering temperature [15–18]. Actually, all these research works have confirmed that the electronic, magnetic, and transport properties are significantly affected by the grain size. Among the earliest reports on the effect of particle size on the physical properties, one can mention that of Mahesh et al. [19], who varied the particle size from 0.025 to 0.35 μm and found significant changes in the properties. Gupta et al. [20] reported that the saturation magnetization decreased with increase in the grain size (grain sizes 3, 14, and 24 μm), although T_c (~230 K) remained constant. However, Zhang et al. [21] observed that T_c decreased with increase in the grain size in the range of 24.4–240 nm. It is known that this variation of T_c is controlled by the electron bandwidth W and the mobility of e_g electrons [11,22,23]. In fact, the structure, magnetism, and the magnetocaloric effect are very correlated, primarily by the bandwidth W .

In addition, our original idea is to change the physical properties by simple methods including simple annealing at low temperature.

It is in this context that the present research work lies to study the effect of the sintering temperature on magnetic and magnetocaloric properties of $\text{La}_{0.8-x}\square_x\text{Ca}_{0.2}\text{MnO}_3$ ($x = 0, 0.1$ and 0.2) manganites.

2. Experimental Details

The $\text{La}_{0.8-x}\square_x\text{Ca}_{0.2}\text{MnO}_3$ ($x = 0, 0.1$ and 0.2) compounds were prepared by solid-state reaction and heated at a temperature of 1373 K. The preparation method as well as the structural and magnetic results were discussed in our previous research work [11]. In the present work, these samples were annealed at 973 K for 7 days in air. The structure of the samples was checked using X-ray diffraction with Cu $K\alpha$ radiation ($\lambda = 1.5406 \text{ \AA}$) by step scanning (0.02°) in the range of $10^\circ \leq 2\theta \leq 100^\circ$. The magnetic measurements were performed on BS2 magnetometer developed in Louis Neel Laboratory of Grenoble.

3. Results and Discussion

The XRD patterns of $\text{La}_{0.8-x}\square_x\text{Ca}_{0.2}\text{MnO}_3$ ($x = 0; 0.1$ and $x = 0.2$) compounds annealed at 973 K are represented in Figure 1. Similarly to the case of the annealing at 1373 K, the refinements of XRD patterns of the compounds annealed at 973 K revealed the presence of two phases. The main phase was accredited to $\text{La}_{0.8-x}\square_x\text{Ca}_{0.2}\text{MnO}_3$, and the other phase was attributed to the presence of unreacted Mn_3O_4 .

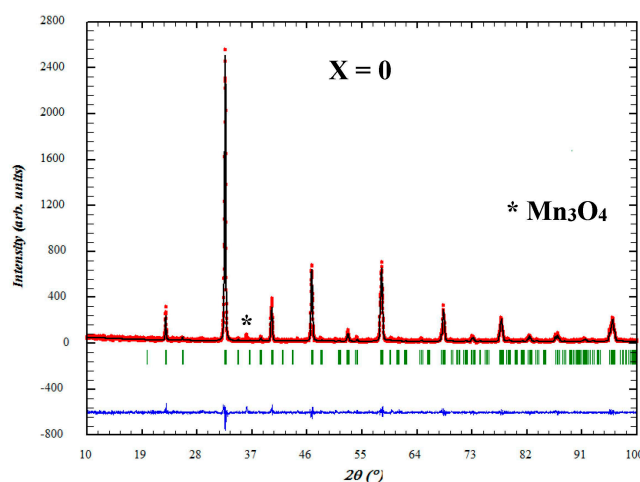


Figure 1. Cont.

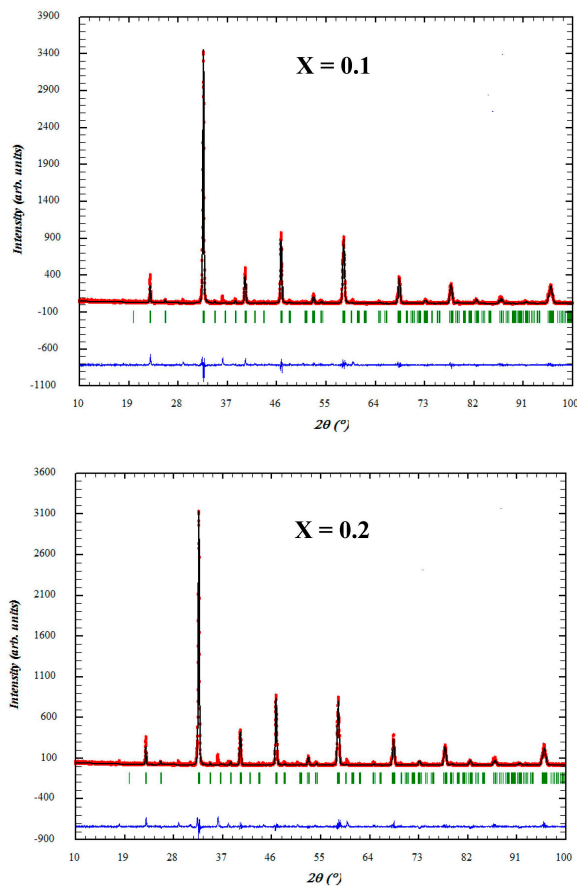


Figure 1. Observed (open symbols) and calculated (solid lines) X-ray diffraction pattern for $\text{La}_{0.8-x}\text{Ca}_{0.2}\text{MnO}_3$ ($x = 0, 0.1$ and 0.2) annealed at 973 K (S2). Positions for the Bragg reflection are marked by vertical bars. Differences between the observed and the calculated intensities are shown at the bottom of the diagram.

The X-ray diffraction analysis showed that all samples crystallized in the orthorhombic structure with Pnma space group.

The results of the refinement are summarized in Table 1. It is worth noting that the decrease of the annealing temperature was accompanied by a reduction of the grain size, leading to a decrease of the bond length $d_{\text{Mn-O}}$, an increase in the bond angle $\theta_{\text{Mn-O-Mn}}$, and thus a decrease in the unit cell volume.

Table 1. Results of Rietveld refinements, determined from XRD patterns recorded at room temperature for $\text{La}_{0.8-x}\text{Ca}_{0.2}\text{MnO}_3$ ($x = 0, 0.1$ and 0.2) compounds annealed at 973 K (S2).

x	0	0.1	0.2
Space group	Pnma	Pnma	Pnma
Lattice parameter			
a (Å)	5.4503	5.448	5.446
b (Å)	7.712	7.709	7.707
c (Å)	5.474	5.468	5.463
Unit cell volume (Å ³)	57.522	57.437	57.412
$d_{\text{Mn-O}}$ (Å)	1.967	1.958	1.952
$\theta_{\text{Mn-O-Mn}}$ (°)	161.234	161.012	160.453
χ^2 (%)	1.27	1.51	1.51

We have also estimated the average crystallite size D from the XRD patterns using the Scherrer formula [8]:

$$D = \frac{180}{\pi} \frac{0.89\lambda}{\beta \cos \theta} \quad (1)$$

where λ is the X-ray wavelength, θ and β are the diffraction angle and the full width for the most intense peak with:

$$\beta = \beta_m^2 - \beta_i^2 \quad (2)$$

β_m^2 is the experimental full width at half maximum (FWHM) and β_i^2 is the FWHM of a standard silicon sample.

The D values were found to be 8.37 nm, 9.23 nm, and 10.48 nm for $x = 0, 0.1$ and 0.2 samples, respectively. In comparison with our previous results [8], it is illustrated that with the increase in the annealing temperature, the particle size of samples increased, confirming that the annealing temperature promotes the grain growth of the samples [15–17,24,25].

It should be mentioned that a special focus was placed on how the physical properties are strongly influenced by the grain size.

Figure 2 displays an example of the temperature dependence (T) of the magnetization (M), measured at the applied magnetic field of 0.05 T, for $\text{La}_{0.8-x}\text{Ca}_{0.2}\text{MnO}_3$ ($x = 0, 0.1$ and 0.2) compounds annealed at 1373 K (S1) and 973 K (S2). For the two annealing temperatures, we can note the presence of a magnetic transition from the ferromagnetic to paramagnetic phase at the Curie temperature T_C , when increasing temperature for S1 and S2 compounds. Moreover, it is clearly shown that the annealing at 973 K induced an increase of the magnetization. The paramagnetic to ferromagnetic (PM–FM) transition temperatures (T_C) were estimated from the peak of dM/dT curves (Figure 3).

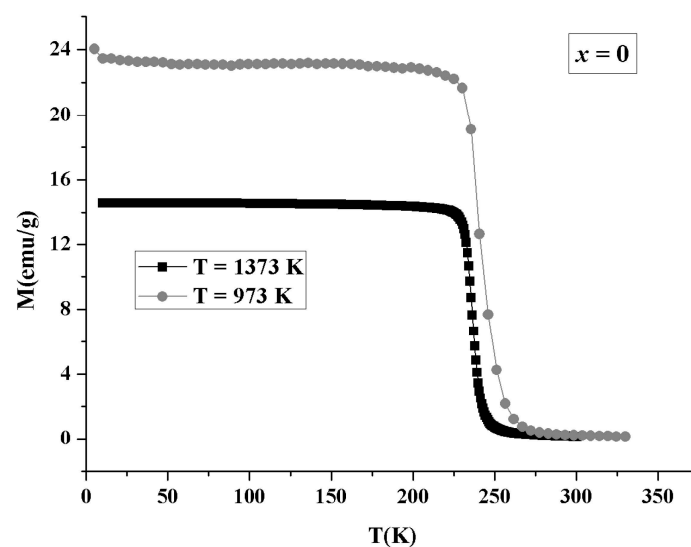


Figure 2. Cont.

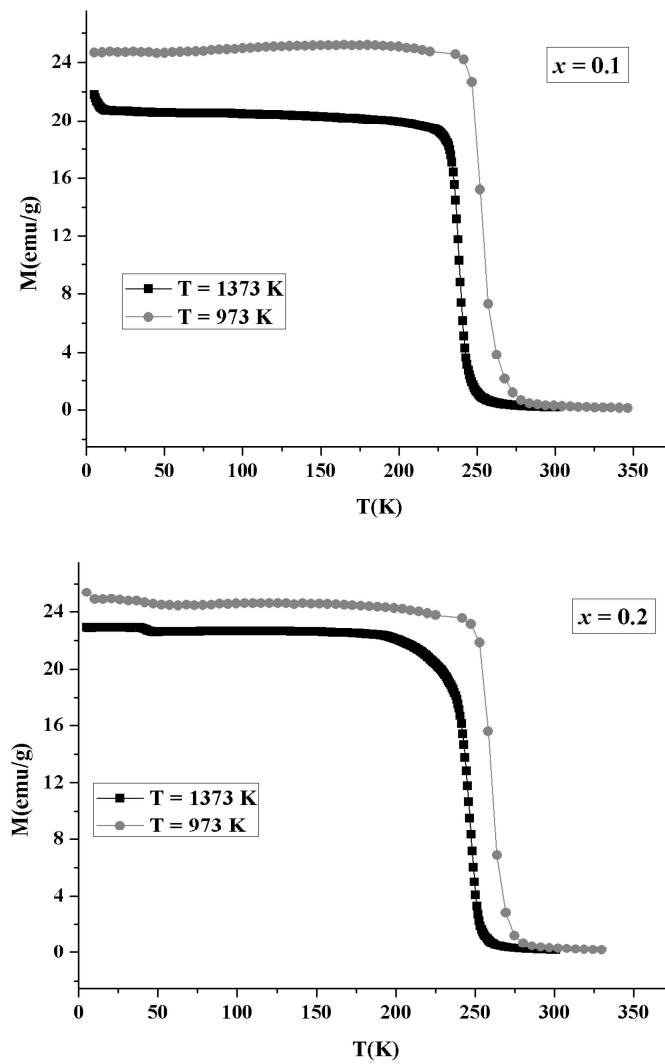


Figure 2. Temperature dependence (T) of the magnetization (M), measured at applied magnetic field of 0.05 T, for $\text{La}_{0.8-x}\text{Ca}_{0.2}\text{MnO}_3$ ($x = 0, 0.1$ and 0.2) compounds annealed at 1373 K (S1) and 973 K (S2).

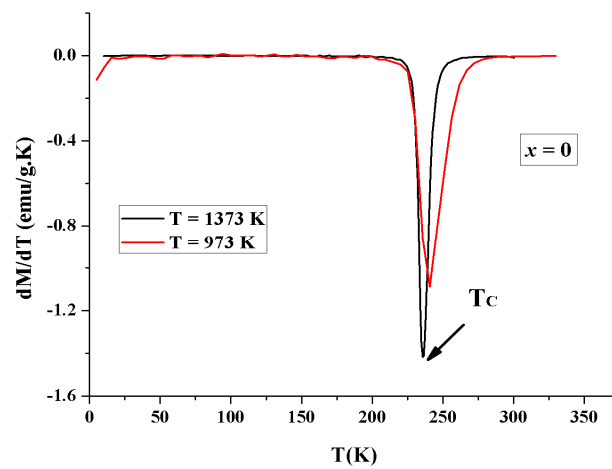


Figure 3. Cont.

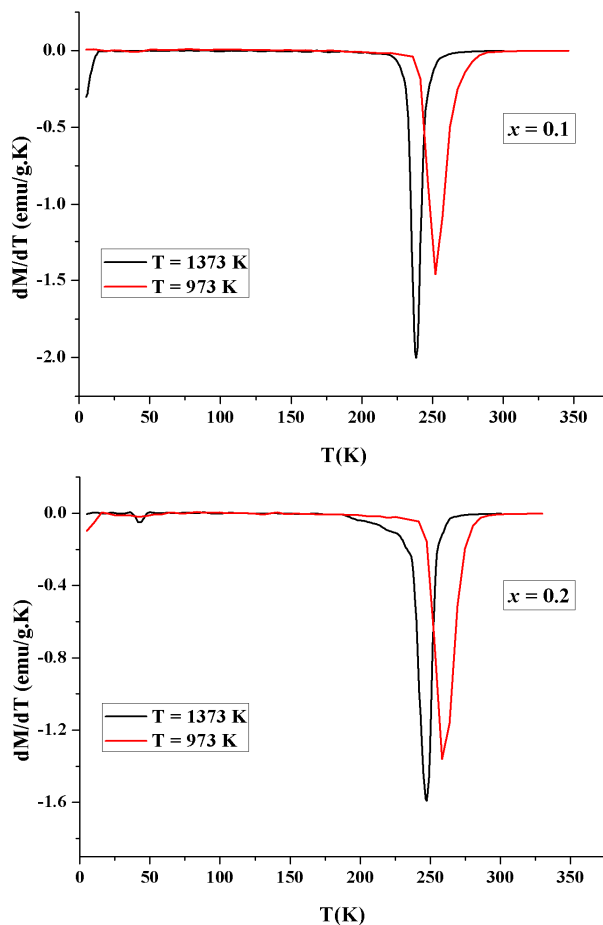


Figure 3. Comparison of the temperature dependence of $(-dM/dT)$ measured for an applied magnetic field of 0.5 T for $La_{0.8-x}Ca_{0.2}MnO_3$ ($x = 0, 0.1$ and 0.2) compounds annealed 1473 K and 973 K.

The decrease of the annealing temperature was found to clearly lead to an important increase of the T_C value. The increase of T_C can be explained by the increase of Mn-O-Mn bond angle and the decrease of Mn-O bond length predictably with the increase of deficiency content. Both shorter Mn-O distance and larger Mn-O-Mn bonding angle lead to the increase of the electron bandwidth W and the mobility of eg electrons, and hence the Double Exchange (DE) interaction (Table 2). Therefore, the improvement of T_C can be explained by the increase of electron-one bandwidth W given by:

$$W = w_0 \frac{\cos\left(\frac{\pi-\gamma}{2}\right)}{\langle d_{Mn-O} \rangle^{3.5}}$$

where γ is the Mn-O-Mn angle, d_{Mn-O} the Mn-O distance, and W_0 a positive constant [26].

Table 2. The Curie temperature (T_C) values for S1 and S2 compounds.

	$T_{\text{annealing}} = 1373 \text{ K}$			$T_{\text{annealing}} = 973 \text{ K}$		
	$x = 0$	$x = 0.1$	$x = 0.2$	$x = 0$	$x = 0.1$	$x = 0.2$
T_C (K)	236	241	247	240	252	258
W/W_0 (10^{-2} eV)	9.05	9.14	9.28	9.361	9.498	9.544

At this level, we were interested in the most important physical property for industrial application—namely the magnetocaloric effect, which is an intrinsic property of magnetic materials. The magnetocaloric effect is a magneto-thermodynamic phenomenon in which a change in temperature of a suitable material is caused by exposing the material to a changing magnetic field. This effect is maximized when the material is near its magnetic ordering temperature (Curie temperature T_C).

Figure 4 shows the magnetic applied field ($\mu_0 H$) dependence of the magnetization $M(T, \mu_0 H)$ measured at different temperatures (T) for the $\text{La}_{0.8-x}\text{Ca}_x\text{MnO}_3$ ($x = 0, 0.1$ and 0.2) compounds annealed at 973 K.

The magnetic entropy change ΔS_M was deduced from the $M(T, \mu_0 H)$ curves using the following equation [27]:

$$\Delta S_M\left(\frac{T_1 + T_2}{2}\right) = \frac{1}{T_2 - T_1} \left[\int_0^{\mu_0 H_{\max}} M(T_2, \mu_0 H) \mu_0 dH - \int_0^{\mu_0 H_{\max}} M(T_1, \mu_0 H) \mu_0 dH \right] \quad (3)$$

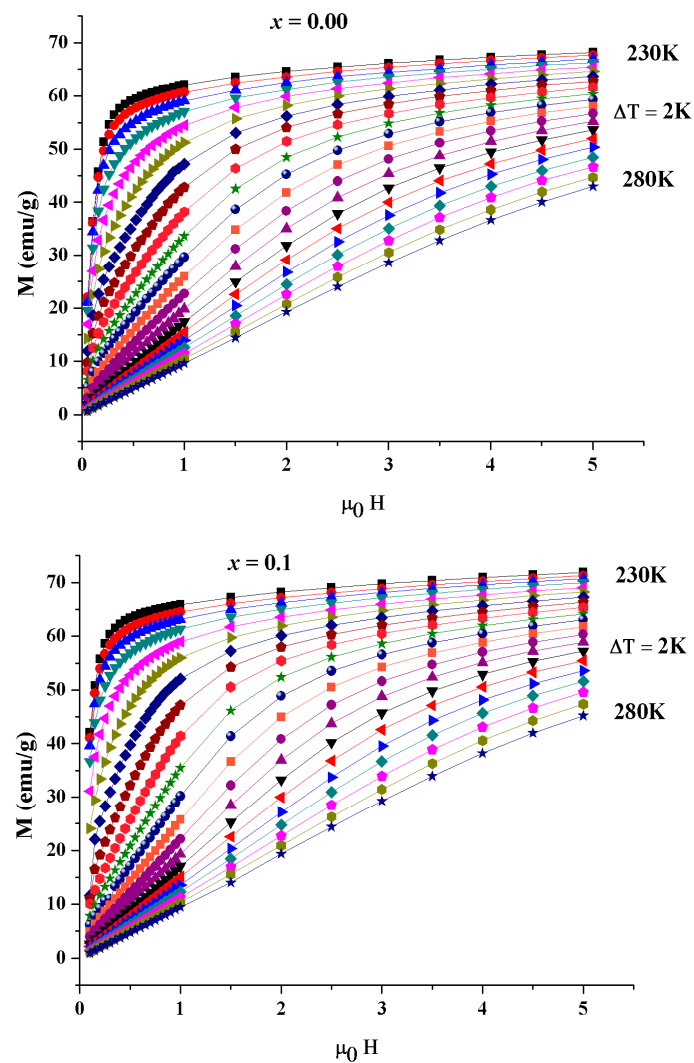


Figure 4. Cont.

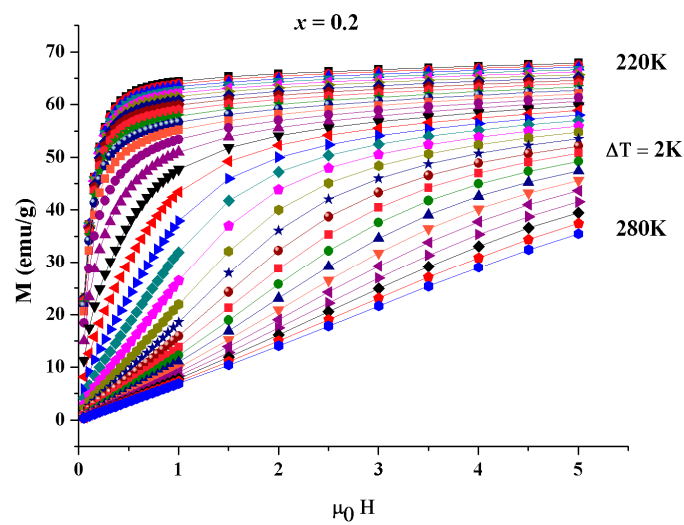


Figure 4. Temperature (T) dependence of the magnetization $M(T, \mu_0H)$ measured at different magnetic applied field (μ_0H) for the $\text{La}_{0.8-x}\text{Ca}_{0.2}\text{MnO}_3$ ($x = 0; 0.1$ and $x = 0.2$) compounds annealed at 973 K.

Figure 5 shows the temperature dependence of the magnetic entropy change ($-\Delta S_M$) measured for an applied magnetic field of 2 T for $x = 0.00$ and 0.2 samples annealed at 1373 and 973 K.

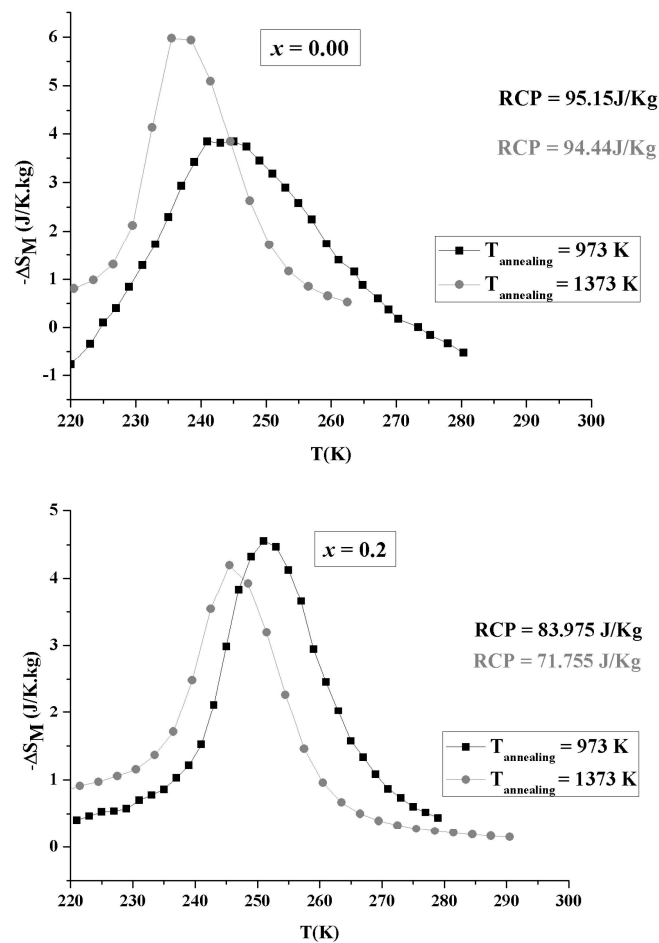


Figure 5. Temperature dependence of the magnetic entropy change ($-\Delta S_M$) measured for an applied magnetic field of 2 T for $x = 0.00$ and 0.2 samples annealed at 1373 and 773K. RCP: relative cooling power.

From these curves, it can be deduced that the annealing at low temperature (973 K) changed the value of the maximum of the magnetic entropy change ($-\Delta S_{M \max}$) and the full width at half maximum (δT_{FWHM}). For example, for $x = 0$, under $H = 2$ T, $\Delta S_{M \max}$ is equal to 5.96 and 3.84 J Kg⁻¹ K⁻¹ at $T_{\text{annealing}} = 1373$ and 973 K, respectively.

The cooling efficiency of magnetic refrigerants was evaluated by means of the so-called relative cooling power (RCP) factor, corresponding to the amount of heat transferred between the cold and hot sinks in the ideal refrigeration cycle and defined as [28]:

$$RCP = -\Delta S_{Max} \times \delta T_{FWHM} \quad (4)$$

where ΔS_{Max} is the maximum of magnetic entropy change and δT_{FWHM} is a full width at half maximum.

We can clearly deduce that the annealing at low temperature (973 K) enhanced the value of the relative cooling power (RCP) factor for both samples (Figure 5).

Table 3 exhibits the comparison between the obtained results and those of other magnetocaloric materials. From the comparison with Gd data and from a technological point of view, our data emphasize that our material can be considered as a relevant potential candidate to be used in cooling systems based on magnetic refrigeration. From an industrial point of view, this material presents beneficial parameters such as low cost, lacking rare earths, low weight, no corrosion, ease of synthesis, and chemical stability. For all these reasons, the suggested material can be considered as a substantial candidate for magnetic refrigeration.

Table 3. Comparison of reported values of the maximum magnetic entropy change ($-\Delta S_{M \max}$) and RCP values at the Curie temperature (T_c) under a magnetic field ($\mu_0 H$) for various manganites and the Gd magnetic refrigerant material.

Materials	T_c (K)	$\mu_0 H$ (T)	$-\Delta S_{M \max}$ (J/K kg)	RCP (J/kg)	References
Gd	299	2	5	196	[29]
La _{0.7} Na _{0.2} MnO ₃	335	2	2.83	76.91	[23]
La _{0.8} Na _{0.15} □ _{0.05} MnO ₃	320	2	2.97	96.06	[23]
La _{0.8} Na _{0.1} □ _{0.1} MnO ₃	295	2	2.97	96.06	[23]
La _{0.8} Ca _{0.2} MnO ₃	240	2	3.84	95.15	This work
La _{0.7} □ _{0.1} Ca _{0.2} MnO ₃	252	2	2.98	96.17	This work
La _{0.6} □ _{0.2} Ca _{0.2} MnO ₃	258	2	4.56	83.97	This work

The change of magnetic entropy can be also calculated from the field dependence of the specific heat by the following integration [30]:

$$\Delta S_M(T, H) = \int_0^T \frac{C_p(T, \mu_0 H) - C_p(T, 0)}{T} dT \quad (5)$$

The change of specific heat ΔC_p associated with a magnetic field variation from 0 to H can be calculated using Equation (5) as:

$$\Delta C_p(T, \mu_0 H) = C_p(T, \mu_0 H) - C_p(T, 0) = \frac{T \delta \Delta S_M(T, \mu_0 H)}{\delta T} \quad (6)$$

Using Equation (6), ΔC_p of the La_{0.8-x}□_xCa_{0.2}MnO₃ ($x = 0$ and 0.2) compounds annealed at 1373 and 973 K versus temperature for an applied magnetic field of 2 T is displayed in Figure 6. As the figure shows, anomalies are observed in all curves around the Curie temperature T_C , due to the magnetic phase transition. The value of ΔC_p undergoes a sudden change of sign from positive to negative around T_C with a negative value below T_C and a positive value above T_C . For example, for $x = 0.2$, the maximum/minimum values of ΔC_p exhibit a steady increase with the decrease of annealing temperature, which proves that the annealing temperature is an alternative method to ameliorate the value of the change of specific heat in manganites.

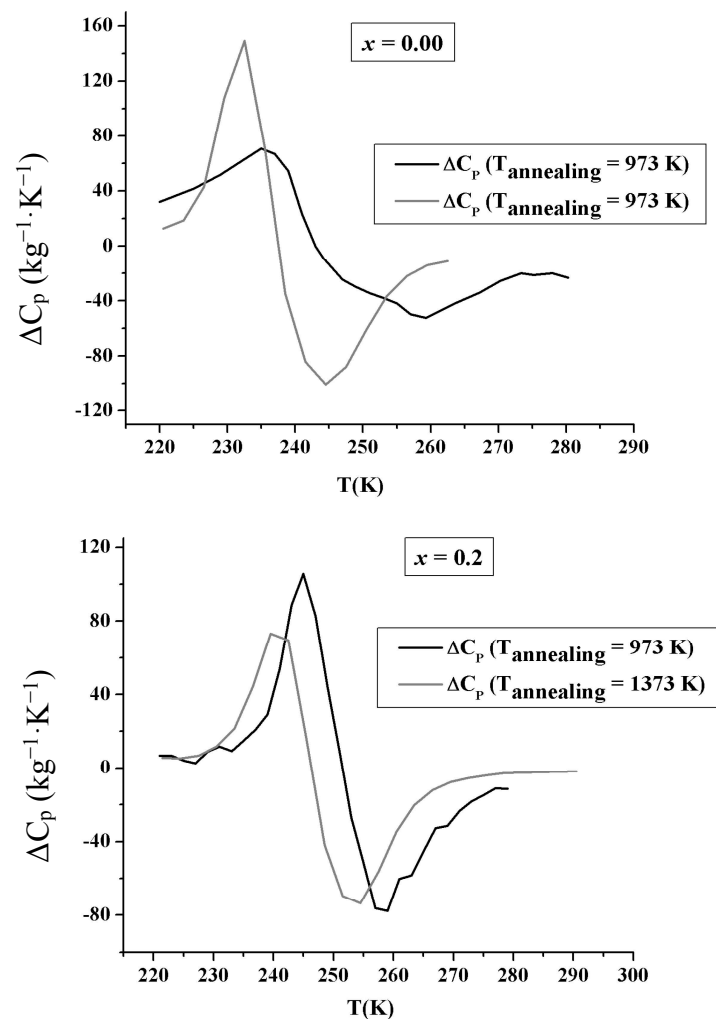


Figure 6. Change of specific heat ΔC_p as a function of temperature calculated for an applied magnetic field of 2 T for $\text{La}_{0.8-x}\text{Ca}_{0.2}\text{MnO}_3$ ($x = 0, 0.1$ and 0.2) samples annealed at 1373 and 773 K.

4. Conclusions

The present work has undertaken the study of the important role of the annealing temperature effects on the structural, magnetic, and magnetocaloric properties of $\text{La}_{0.8-x}\text{Ca}_{0.2}\text{MnO}_3$ ($x = 0; 0.1$ and $x = 0.2$) samples. The decrease of the annealing temperature from 1373 (S1) to 973 K (S2) was found to decrease the grain size, leading to: (i) a decrease of the lattice parameters and the unit cell volume, (ii) an increase of magnetization as well as of Curie Temperature T_c , (iii) an increase of the value of the (RCP) factor.

Acknowledgments: This paper is supported by the Tunisian Ministry of Higher Education and Scientific Research.

Author Contributions: Ridha Skini analyzed the data and wrote the paper, Hlil El Kebir performed the experiments, Essebti Dhahri provided with the samples.

Conflicts of Interest: The authors declare no conflict of interest.

References

1. Tishin, A.M.; Spichkin, Y.I. *The Magnetocaloric Effect and Its Applications*; IOP Publishing Ltd.: Bristol, UK, 2003.
2. Mira, J.; Rivas, J.; Rivadulla, F.; Vázquez-Vázquez, C.; López-Quintela, M.A. Change from first- to second-order magnetic phase transition in $\text{La}_{2/3}(\text{Ca,Sr})_{1/3}\text{MnO}_3$ perovskites. *Phys. Rev. B* **1999**, *60*, 2998. [[CrossRef](#)]

3. Chahara, K.; Ohno, T.; Kasai, M.; Kozono, Y. Magnetoresistance in magnetic manganese oxide with intrinsic antiferromagnetic spin structure. *Appl. Phys. Lett.* **1993**, *63*, 1990. [[CrossRef](#)]
4. Von Helmolt, R.; Wecker, J.; Holzapfel, B.; Schultz, L.; Samwer, K. Giant negative magnetoresistance in perovskitelike $\text{La}_{2/3}\text{Ba}_{1/3}\text{MnO}_x$ ferromagnetic films. *Phys. Rev. Lett.* **1993**, *71*, 2331. [[CrossRef](#)] [[PubMed](#)]
5. McCormack, M.; Jin, S.; Tiefel, T.H.; Fleming, R.M.; Phillips, J.M.; Ramesh, R. Very large magnetoresistance in perovskite-like La-Ca-Mn-O thin films. *Appl. Phys. Lett.* **1994**, *64*, 3045. [[CrossRef](#)]
6. Jin, S.; Tiefel, T.H.; McCormack, M.; Fastnacht, R.A.; Ramesh, R.; Chen, L.H. Thousandfold change in resistivity in magnetoresistive La-Ca-Mn-O films. *Science* **1994**, *264*, 413. [[CrossRef](#)] [[PubMed](#)]
7. Khlifi, M.; Dhahri, E.; Hlil, E.K. Magnetic, magnetocaloric, magnetotransport and magnetoresistance properties of calcium deficient manganites $\text{La}_{0.8}\text{Ca}_{0.2-x}\square_x\text{MnO}_3$ post-annealed at 800 °C. *J. Alloys. Compd.* **2014**, *587*, 771–777. [[CrossRef](#)]
8. Skini, R.; Khlifi, M.; Wali, M.; Dhahri, E.; Hlil, E.K.; Lachkar, P. Electrical transport and giant magnetoresistance in $\text{La}_{0.8-x}\square_x\text{Ca}_{0.2}\text{MnO}_3$ ($x=0, 0.1$ and 0.2) oxides. *J. Magn. Magn. Mater.* **2014**, *363*, 217–223. [[CrossRef](#)]
9. Lu, W.J.; Luo, X.; Hao, C.Y.; Song, W.H.; Sun, Y.P. Magnetocaloric effect and Griffiths-like phase in $\text{La}_{0.67}\text{Sr}_{0.33}\text{MnO}_3$ nanoparticles. *J. Appl. Phys.* **2008**, *104*, 113908. [[CrossRef](#)]
10. Bingham, N.S.; Phan, M.H.; Srikanth, H.; Torija, M.A.; Leighton, C. Magnetocaloric effect and refrigerant capacity in charge-ordered manganites. *J. Appl. Phys.* **2009**, *106*, 023909. [[CrossRef](#)]
11. Skini, R.; Omri, A.; Khlifi, M.; Dhahri, E.; Hlil, E.K. Large magnetocaloric effect in lanthanum-deficiency manganites $\text{La}_{0.8-x}\square_x\text{Ca}_{0.2}\text{MnO}_3$ ($0.00 \leq x \leq 0.20$) with a first-order magnetic phase transition. *J. Magn. Magn. Mater.* **2014**, *364*, 5–10. [[CrossRef](#)]
12. Nisha, P.; Pillai, S.S.; Darbandi, A.; Misra, A.; Suresh, K.G.; Varma, M.R.; Hahn, H. Magnetism and magnetocaloric effect in nanocrystalline $\text{La}_{0.67}\text{Ca}_{0.33}\text{Mn}_{0.9}\text{V}_{0.1}\text{O}_3$ synthesized by nebulized spray pyrolysis. *J. Phys. D Appl. Phys.* **2010**, *43*, 135001. [[CrossRef](#)]
13. Tang, W.; Lu, W.; Luo, X.; Wang, B.; Zhu, X.; Song, W.; Yang, Z.; Sun, Y. Particle size effects on $\text{La}_{0.7}\text{Ca}_{0.3}\text{MnO}_3$: Size-induced changes of magnetic phase transition order and magnetocaloric study. *J. Magn. Magn. Mater.* **2010**, *322*, 2360–2368. [[CrossRef](#)]
14. Khlifi, M.; Bejar, O.; Sadek, E.L.; Dhahri, E.; Ahmed, M.A.; Hlil, E.K. Structural, magnetic and magnetocaloric properties of the lanthanum deficient in $\text{La}_{0.8}\text{Ca}_{0.2-x}\square_x\text{MnO}_3$ ($x = 0-0.20$) manganites oxides. *J. Alloys Compd.* **2011**, *509*, 7410–7415. [[CrossRef](#)]
15. Dey, P.; Nath, T.K. Effect of grain size modulation on the magneto- and electronic-transport properties of $\text{La}_{0.7}\text{Ca}_{0.3}\text{MnO}_3$ nanoparticles: The role of spin-polarized tunneling at the enhanced grain surface. *Phys. Rev. B* **2006**, *73*, 214425. [[CrossRef](#)]
16. Dutta, A.; Gayathri, N.; Ranganathan, R. Effect of particle size on the magnetic and transport properties of $\text{La}_{0.875}\text{Sr}_{0.125}\text{MnO}_3$. *Phys. Rev. B* **2003**, *68*, 054432. [[CrossRef](#)]
17. Othmani, S.; Bejar, M.; Dhahri, E.; Hlil, E.K. The effect of the annealing temperature on the structural and magnetic properties of the manganites compounds. *J. Alloys Compd.* **2009**, *475*, 46–50. [[CrossRef](#)]
18. M'nassri, R.; Chniba Boudjada, N.; Cheikhrouhou, A. Impact of sintering temperature on the magnetic and magnetocaloric properties in $\text{Pr}_{0.5}\text{Eu}_{0.1}\text{Sr}_{0.4}\text{MnO}_3$ manganites. *J. Alloys Compd.* **2015**, *626*, 20–28. [[CrossRef](#)]
19. Mahesh, R.; Mahendiran, R.; Raychaudhuri, A.K.; Rao, C.N.R. Effect of particle size on the giant magnetoresistance of $\text{La}_{0.7}\text{Ca}_{0.3}\text{MnO}_3$. *Appl. Phys. Lett.* **1996**, *68*, 2291. [[CrossRef](#)]
20. Gupta, A.; Gong, G.Q.; Xiao, G.; Duncombe, P.R.; Lecoer, P.; Trouilloud, P.; Wang, Y.Y.; David, V.P.; Sun, J.Z. Grain-boundary effects on the magnetoresistance properties of perovskite manganite films. *Phys. Rev. B* **1996**, *54*, R15629. [[CrossRef](#)]
21. Zhang, N.; Ding, W.; Zhong, W.; Xing, D.; Duet, Y. Tunnel-type giant magnetoresistance in the granular perovskite $\text{La}_{0.85}\text{Sr}_{0.15}\text{MnO}_3$. *Phys. Rev. B* **1997**, *56*, 8138. [[CrossRef](#)]
22. Skini, R.; Khlifi, M.; Hlil, E.K. An efficient composite magnetocaloric material with a tunable temperature transition in K-deficient manganites. *RSC Adv.* **2016**, *6*, 34271–34279. [[CrossRef](#)]
23. Wali, M.; Skini, R.; Khlifi, M.; Dhahri, E.; Hlil, E.K. A giant magnetocaloric effect with a tunable temperature transition close to room temperature in Na-deficient $\text{La}_{0.8}\text{Na}_{0.2-x}\square_x\text{MnO}_3$ manganites. *J. Dalton. Trans.* **2015**, *44*, 12796–12803. [[CrossRef](#)] [[PubMed](#)]

24. Baaziz, H.; Maaloul, N.K.; Tozri, A.; Rahmouni, H.; Mizouri, S.; Khirouni, K.; Dhahri, E. Effect of sintering temperature and grain size on the electrical transport properties of $\text{La}_{0.67}\text{Sr}_{0.33}\text{MnO}_3$ manganite. *J. Chem. Phys. Lett.* **2015**, *640*, 77–81. [[CrossRef](#)]
25. Zhou, Y.; Zhu, X.; Li, X. Effect of particle size on magnetic and electric transport properties of $\text{La}_{0.67}\text{Sr}_{0.33}\text{MnO}_3$ coatings. *Phys. Chem. Chem. Phys.* **2015**, *17*, 31161. [[CrossRef](#)] [[PubMed](#)]
26. Radaelli, P.G.; Iannone, G.; Marezio, M.; Hwang, H.Y.; Cheong, S.-W.; Jorgensen, J.D.; Argyriou, D.N. Structural effects on the magnetic and transport properties of perovskite $\text{A}_{1-x}\text{A}'_x\text{MnO}_3$ ($x = 0.25, 0.30$). *Phys. Rev. B* **1997**, *56*, 8265–8276. [[CrossRef](#)]
27. Foldcaki, M.; Chahine, R.; Gopal, B.R.; Bose, T.K. Investigation of the magnetic properties of the $\text{Gd}_{1-x}\text{Er}_x$ alloy system in the $x < 0.62$ composition range. *J. Magn. Magn. Mater.* **1995**, *150*, 421–429.
28. Gschneidner, K.A., Jr.; Pecharsky, V.K. Magnetocaloric Materials. *Ann. Rev. Mater. Sci.* **2000**, *30*, 387–429. [[CrossRef](#)]
29. Pecharsky, V.K.; Gschneidner, K.A., Jr. Giant Magnetocaloric Effect in $\text{Gd}_5(\text{Si}_2\text{Ge}_2)$. *Phys. Rev. Lett.* **1997**, *78*, 4494. [[CrossRef](#)]
30. Phan, M.H.; Yu, S.C. Review of the magnetocaloric effect in manganite materials. *J. Magn. Magn. Mater.* **2007**, *308*, 325–340. [[CrossRef](#)]



© 2017 by the authors. Licensee MDPI, Basel, Switzerland. This article is an open access article distributed under the terms and conditions of the Creative Commons Attribution (CC BY) license (<http://creativecommons.org/licenses/by/4.0/>).